Yu *et al.*
Chinese Journal of Mechanical Engineering (2023) 36:88
https://doi.org/10.1186/s10033-023-00916-3

ORIGINAL ARTICLE **Open Access**

Direct-Ink-Writing Printed Strain Rosette Sensor Array with Optimized Circuit Layout

Peishi Yu[1,2], Lixin Qi[1,2], Zhiyang Guo[1,2], Yu Liu[1,2] and Junhua Zhao[1,2*]

Abstract

The full-field multiaxial strain measurement is highly desired for application of structural monitoring but still challenging, especially when the manufacturing and assembling for large-area sensing devices is quite difficult. Compared with the traditional procedure of gluing commercial strain gauges on the structure surfaces for strain monitoring, the recently developed Direct-Ink-Writing (DIW) technology provides a feasible way to directly print sensors on the structure. However, there are still crucial issues in the design and printing strategies to be probed and improved. Therefore, in this work, we propose an integrated strategy from layered circuit scheme to rapid manufacturing of strain rosette sensor array based on the DIW technology. Benefit from the innovative design with simplified circuit layout and the advantages of DIW for printing multilayer structures, here we achieve optimization design principle for strain rosette sensor array with scalable circuit layout, which enable a hierarchical printing strategy for multiaxial strain monitoring in large scale or multiple domains. The strategy is highly expected to adapt for the emerging requirement in various applications such as integrated soft electronics, nondestructive testing and small-batch medical devices.

Keywords Direct-ink-writing, Strain rosette sensor array, Layered circuit scheme, Printing strategy

1 Introduction

The direct-ink-writing (DIW) is one of the promising additive manufacturing technologies and recognized as a versatile way to rapidly construct complex 3D structures through continuously extruding various functional slurries [1–4]. Based on a computer-controlled moving platform, the designed structures can be directly stacked layer by layer through converting the coordinate information of the designed scheme into printing codes [5–8]. Compared with traditional 3D printing technologies such as light curing and laser melting, the DIW is flexible and suitable for various functional pastes/inks composed of polymer and nano/micro conductive particles. Therefore, it is widely used to fabricate various novel sensors [9–12], and show significant advantages comparing with the screen/stencil printing [13–16] and spray coating [17, 18]. Strain sensor for structural monitoring needs to be integrated with the substrate. The widely used solution is to paste the sensor on the specific position of the detected component, which requires manual operation, with inherent low positioning accuracy, efficiency and durability. In comparisions with the various new manufacturing technologies of the sensor [16, 18, 19], the DIW directly prints the sensing materials on the structural surface according to the design scheme. Therefore, the manufacturing and installation of the sensor can be completed in one step, eliminating various disadvantages caused by the manual pasting. In addition, the DIW printing simplifies the fabrication process, thus has unique advantages in personal-demanded sensors in small-batch, or conceptual proof of rapid iterative design.

*Correspondence:
Junhua Zhao
junhua.zhao@163.com
[1] Jiangsu Key Laboratory of Advanced Food Manufacturing Equipment and Technology, School of Mechanical Engineering, Jiangnan University, Wuxi 214122, China
[2] Jiangsu Province Engineering Research Center of Micro-Nano Additive and Subtractive Manufacturing, Institute of Advanced Technology, Jiangnan University, Wuxi 214122, China

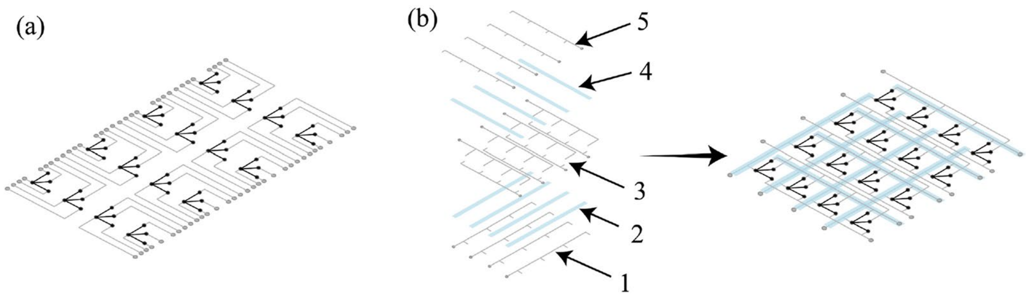

Figure 1 Circuit layout of (**a**) traditional circuit layout and (**b**) developed multilayer design for the strain rosette array composed of 4 × 4 units

Among the various sensors for detecting different physical quantities, the strain sensor has been extensively developed and widely used for mechanical engineering. For instance: Madhavan [20] desgined an epidermis-like strain sensor for monitoring human activities; Ma et al. [21] printed fast-response and ultra-sensitive strain sensors using okra polysaccharide-based hydrogel; Liu et al. [22] used the graphene-based hydrogel to print strain sensors with breathability for motion detection; He et al. [23] probed a high sensitive strain sensor based on micro-helix micro taper long period fiber grating; Wang et al. [24] used nanofibrillated cellulose to obtain a lipase induced highly hydrophobic film for strain sensors; Dong et al. [25] prepared wearable strain sensor based on PVA/MWCNTs hydrogel composite; Zhang et al. [26] focused on the high gauge factors under small strains using antibacterial HPMC-anchored conductive polymer composite. Accordingly, the DIW is also adapted to achieve novel strain sensors with improved performance including higher gauge factor ($GF \geq 10$) and larger stretchability ($\varepsilon_{\max} \geq 20\%$) [23, 27, 28] than those of traditional metal foil strain gauge (i.e., $GF \leq 2$ and $\varepsilon_{\max} \leq 2\%$, in general). The performance of the sensor depends on not only the material performance, but also the design scheme and process parameters. In our previous work, the dependence between structure and performance has been explored: the design model of typical sandwich structure sensor has been established, based on which the influence of layer thickness and material elastic constant of structure on interlayer strain transfer has been accurately predicted [28]; the quantitative dependence of the sensor interlayer strength on the layer thickness is predicted by using the interfacial mechanics theory and cohesion model [29]. Based on the design model and optimized printing process for independent sensor unit, we propose a bi-material strategy to print the sensing unit by carbon paste and the connecting wires by silver paste, respectively [30]. Accordingly, we develop a simplified circuit layout of uniformly-orientated sensor arrays, which successfully monitor uniaxial strains with the same direction of sensors.

Although the traditional multi-step lithography method can be used to prepare such layered circuit, the DIW technology are still featured by two significant advantages, i.e., low cost and rapid individual fabrication. For one thing, the DIW directly converts the design scheme into real sensor array in low cost without preparing the expensive patterned mold which is necessary for the lithography method. For another, the DIW achieves rapid realization from individual designed scheme to specific application requirement. Due to the merit of the DIW technology, it is expected to applied in the non-batch fabrication for complex circuit layout of individual sensing requirement. In order to monitor the full-field strain of complex stress state, the sensor array with strain rosettes is needed to measure the strain components in different directions. Therefore, in this work, we develop a layered circuit for the strain arrays with optimized design diagram. Based on the proposed design diagram, the electrodes and wires consumption in the circuit are significantly reduced. The array circuit layout is scalable, which enable hierarchical printing for large area or multiple domains. Then a simple strain rosette sensor array is printed and high precision multiaxial strain field are monitored under remote tensile loading. The developed design diagram and printing strategy for the strain rosette sensor array is highly expected to extend for various applications especially for monitoring small-batch equipment with complex strain state.

2 Optimization Design for the Strain Rosette Array with Multilayer Circuit

2.1 Simplification Design of the Strain Rosette Sensor Array

The multi-axis strain rosette is composed of three sensors with the directions of 0, 45° and 90°. When the array includes a large number of independent units, the traditional circuit design will become very complex (as shown in Figure 1a), and finally causes the inconvenient printing

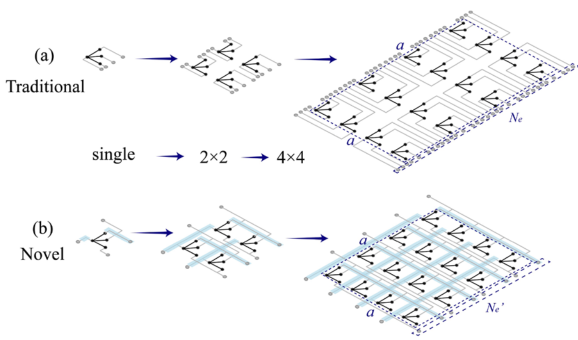

Figure 2 Simplicity analysis of (**a**) traditional and (**b**) novel circuit layout

for technology. In addition, the abundant wires accumulate in a tight space and occupy the printable area of the sensing unit in the limited monitoring field. Therefore, we propose a multilayer design strategy, which arranges common electrodes and wires to simplify the circuit layout, as shown in Figure 1b. Different from the traditional sensor array composed of independent units within one single layer, the novel design contains 5 layers, thereby compresses the area occupation for the electrodes and wires in the circuit layout. The wires are designed in the 1st, 3rd, and 5th layers, and the cross intersections among different layers are insulated by the printed alternating strips between the adjacent circuit layers. To avoid the signal interference induced by the public wires and extrudes, a data acquisition system with multiplexer is used to distinguish resistance variation for each unit by high-frequency scanning on the whole circuit in combination with equipotential shielding for the circuit channels.

The simplification of the multilayer design is quantified by the reduction of electrodes number (defined by N_e for the traditional circuit and N_e' for the multilayer design, respectively). The comparison of the complexity between the traditional and developed circuit is shown in Figure 2. The results show the advantages of the novel design for reducing the electrodes and compacting the integration of sensor units.

The relationship of electrodes number with row number of the array is inducted based on Figure 2 and shown in Eq. (1) as follows:

$$\left[N_\mathrm{e} \ N_\mathrm{e}' \right] = \left[4n^2 \ 4n \right]. \tag{1}$$

Then the ratio of the extrudes numbers is expressed by Eq. (2), and quantified in Figure 3, which shows a significant improvement of the proposed design in electrode number with the increasing capacity,

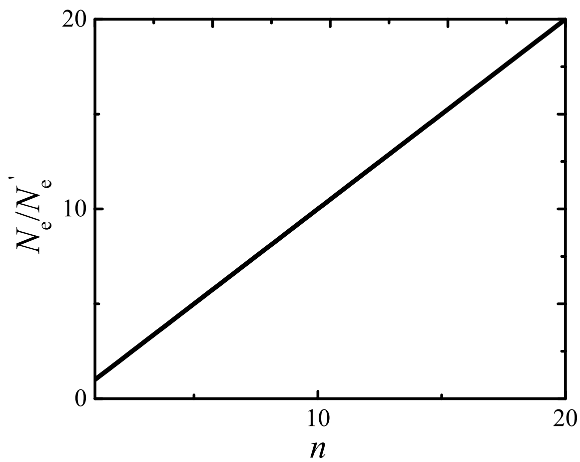

Figure 3 Ratio of electrodes $N_\mathrm{e}/N_\mathrm{e}'$ between the traditional and multilayer designs

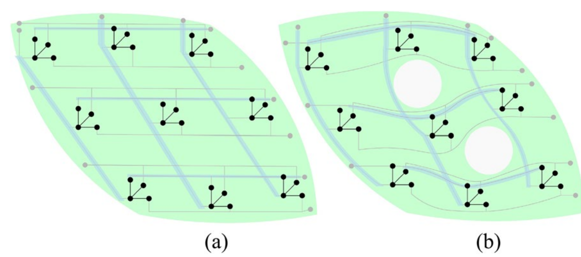

Figure 4 Adaptability of the strain rosette sensor arrays for arbitrary-shaped (**a**) simple connected and (**b**) multi connected domain

$$N_\mathrm{e} / N_\mathrm{e}' = n. \tag{2}$$

2.2 Adaptability and Scalability of the Simplified Circuit Layout for the Strain Rosette Sensor Array

High adaptability is desired for monitoring domain with arbitrary shape. As shown in Figure 4, the proposed printing model can be arbitrarily arranged in simple and multi connected areas with good adaptability, respectively. Benefit from the programmed printing path with high flexibility, the DIW provides an efficient strategy for strain monitoring of irregular shapes, especially when screen printing or lithography are difficult or too expensive for preparing the templates.

In addition, once the traditional design scheme is fabricated, it is technically difficult to expand the array because the insufficient area required for extra electrodes and wires. For the optimized design strategy, the scalability of the circuit is significantly improved, as shown in Figure 5.

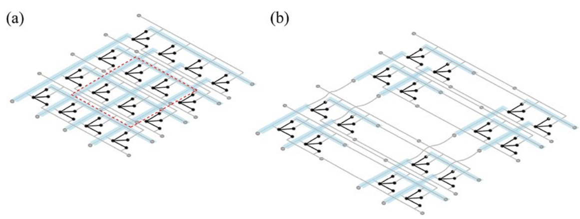

Figure 5 Two typical strategies for scalable strain rosette sensor array: (**a**) Through expanding the basic circuit layout, (**b**) By connecting the electrodes of separated sensor arrays orderly

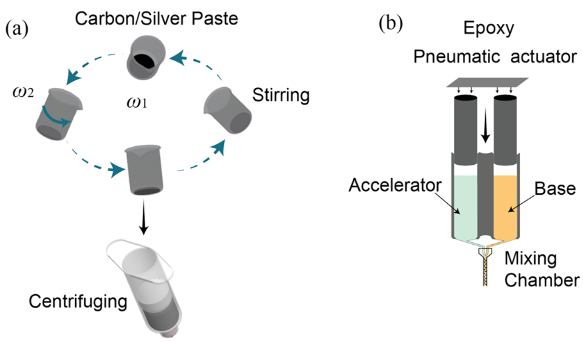

Figure 6 Preparation for (**a**) carbon/silver paste and (**b**) epoxy

Firstly, a circuit layout composed of 2 × 2 units is designed according to the novel scheme. Secondly, we duplicate the unit and expand the circuit to directly achieve a larger 4 × 4 strain rosette sensor array, as shown in Figure 5a. Besides, we print four separated 4 × 4 arrays, and then connect the adjacent electrodes to obtain a larger array composed of 4 × 4 units as shown in Figure 5b. Accordingly, the high scalability also leads to a hierarchical printing strategy to match for larger area exceeding the range of platform of motion platform.

3 Fabrication for the Design Schemes and Experimental Validation

3.1 Preparing for the Materials and Typical Samples Printing

We use the carbon paste CH-8/MOD2 (resistivity $\rho = 1.0 \times 10^{-2}$ Ω·cm) and silver paste EN-06B8 (resistivity $\rho \le 8 \times 10^{-5}$ Ω·cm) to print the unit and wires in the strain rosette sensor array, respectively. The preparations for the two inks are inherited from the previous works [28–30]. The insulation base, insulation strips and coating layer are printed using bi-component epoxy resin (DP190, 3M). The base and accelerator with a weight ratio of 1:1 is extruded by pressure to a zigzag-channel chamber, in which the epoxy mixed thoroughly, as shown in Figure 6.

Among the several rheological parameters, viscosity is a dominated factor for the printability and forming quality. Therefore, here we provide detailed viscosities

Table 1 Optimized process parameters for printing strain rosette sensor

Inks	Diameter of nozzle (mm)	Air pressure (MPa)	Printing speed (mm/s)	Curing parameters
Epoxy	0.26	0.125	10	2 h at 71 ℃
Silver paste	0.21	0.25	7	30 min at 75 ℃
Carbon paste	0.21	0.25	7	2 h at 80 ℃

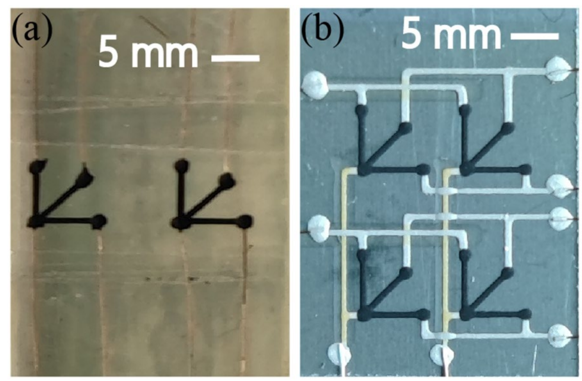

Figure 7 Samples for the DIW printed (**a**) separated strain rosettes and (**b**) arrays with 2 × 2 units

of the three used inks for the sensor units, wires and isolations in the array circuit. The base viscosities at room temperature (25 ℃) of the carbon paste (CH-8(MOD2), JELCON), silver paste (EN-06B8) and epoxy resin (DP190, 3M) are 30000 ± 6500 mPa·s, 260 ± 50 mPa·s and 2000–8000 mPa·s, respectively.

The printing is carried out using an air pulse dispenser (ML-5000XII-CTR, MUSASHI). The process parameters are also inherited from our previous works [28–30] with the details in Table 1.

Based on the printing process parameters, two typical samples are fabricated through a syringe controlled by a programed motion platform, as shown in Figure 7. The two independent strain rosettes in Figure 7a is used to calibrate *GF* for each unit.

The interfacial strength is really important especially for the multilayer sensor array with hetero-composite structure. In our previous works, we have systematically designed and tested the strain transition and interfacial strength between different layers, which demonstrated high robustness of the interfaces among different layers from the metal substrate to covering layer [28, 29]. Here, we just inherited the previous materials and hetero-composite structure for the sensor unit. As a consequence, it is reasonably concluded that the robust interface would

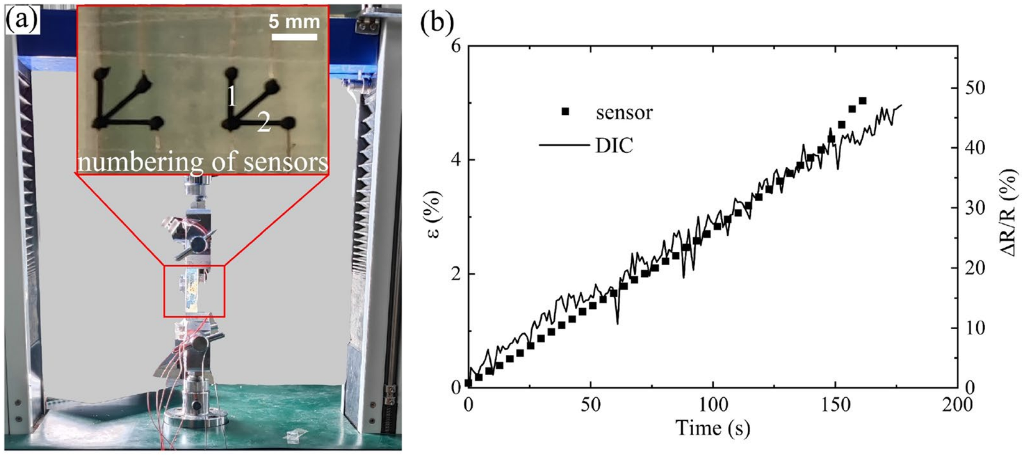

Figure 8 Calibration of *GF* for the printed strain rosette sensor: (**a**) Specimen with separated strain rosette clamped on the test machine, (**b**) Strain measured by DIC and the resistance variation recorded by the sensor unit

be maintained in the strain rosette sensor arrays, due to the consistent multi-layer structure of same materials.

3.2 Experimental Validation of the Printed Strain Rosette Sensor Array for Monitoring Strain-Field

The *GF* for each branch of the strain rosette is calibrated based on the specimen shown in Figure 7a. The *GF* is calculated by $GF = (\Delta R/R)/\varepsilon$, where ΔR is the resistance change caused by the deformation of the base and measured by data acquisition system (KEYSIGHT DAQ970A), R is the resistance of strain sensor before deformation, and ε is the strain. ε is measured by digital image correlation (DIC, GOM Correlate Professional) instrument. The specimen and loading setup are shown in Figure 8a, while the recorded resistance variation of one representative branch and the captured strain by DIC at the back of the specimen are shown in Figure 8b. The *GF* is determined by the ratio of $\Delta R/R$ measured by sensor unit to the strain ε recorded by DIC. Based on the test data in Figure 8b, the *GF* is calibrated as 9 (the ratio of right $\Delta R/R$ data to the left ε data) with a well linearity for $\varepsilon \leq 4$ %. By comparison with the represent works of extrusion-printed sensors [31–33], it is found that the performance of the sensor unit is comparable in the *GF* and linearity.

We print a 2×2 strain rosette sensor array on a 304L stainless steel sheet and then demonstrate the application for monitoring the strain. The strains in the back side are captured by the DIC instrument. The specimen is loaded under quasi-static tensile using the MTS testing system. During the loading process, the data acquisition system (DAQ970A) and DIC instrument simultaneously measure the strain field on the front and back sides of the specimen during the loading process. The loading set up, the strain rosette sensor array and DIC-speckle are indicated in Figure 9a–c. The strain data at the six marked branches of two sensor rosette units in Figure 9b are measured, which show high agreement with those recorded by the DIC, as summarized in Figure 9d, e. The strain data monitored by the printed strain rosette sensor array show significant directional dependency. The strain values measured for the same direction show high agreement, which imply the consistency of the sensor units. Besides, branch 1 and 2 represent the first principal strain along the remote loading direction, whereas the strains in branch 3 and 4 are negative due to the Poisson's effect. The strains in branch 5 and 6 are positive and about half of branch 1 and 2, which is consistent with the prediction by the conversion relationship between different directions.

The cyclic durability performance is crucial for practical applications. In a parallel work [34], we preliminarily tested the performance evolution for the DIW-based strain sensor under fatigue loading, which show acceptable durability for the printed sensors under large strain 3.25% under more than 10^5 cycles. Although the durability performance of the sensor unit is not exactly equivalent to that of the sensor array, it is still expected to be a reference. Moreover, in-depth study for the durability of the DIW-based sensor array is necessary, but still need to develop lots of testing technologies. For example, in order to avoid mutual interference in the sensor array, the commercial data acquisition system (KEYSIGHT DAQ970A) is adopted to activate each circuit ergodically with the maximum frequency of 100 Hz. For quasi static loading, the change of resistance for each sensor unit can be well recorded. However, when the fatigue loading with moderate frequency is applied on the sensor array containing numerous sensor units, it is quite difficult to

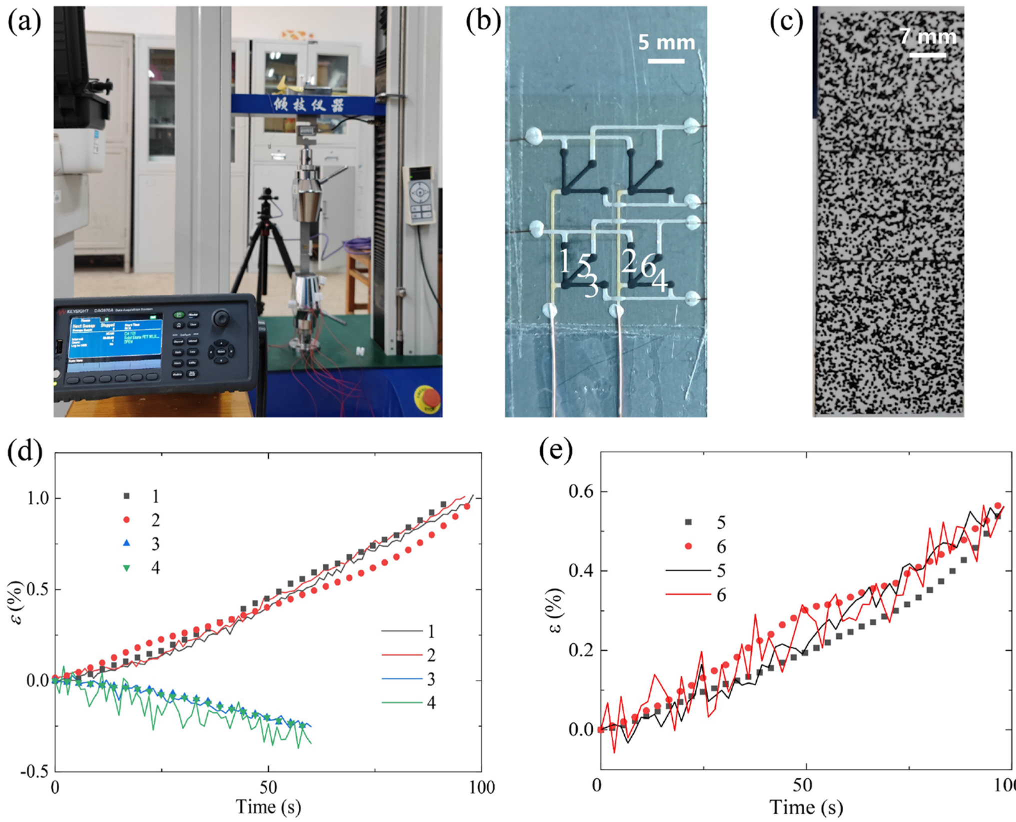

Figure 9 Strain monitoring for a specimen based on the printed strain rosette sensor array: (**a**) Testing set up, (**b**) and (**c**) Two sides of the specimen attached by the printed strain rosette sensor array and DIC-speckle, (**d**) and (**e**) Real-time recording strain data at the six marked branches monitored by the printed strain rosette sensor array and the data extracted from the DIC

record enough data points for each unit to record a full waveform in one cycle of short period. To address this limitation of the commercial instrument, we are trying to develop a testing system to achieve much higher ergodic frequency in an ongoing work.

4 Conclusions

(1) The design diagram, fabrication strategy and application for the DIW printed strain rosette sensor array are systematically studied. By introducing a multilayer strategy, a new design principle is developed, which significantly optimize the circuit layout of the sensor array with high adaptability and scalability.
(2) A hierarchical printing strategy is probed to assemble independent small arrays to form a uniform large array for monitoring of large-scale regions or multiple domains. Based on the design conception, the DIW printing and testing validation for the printed strain rosette sensor array are further demonstrated, which shows potential applications of the proposed design principles and manufacturing strategies.
(3) It is expected to provides a feasible solution for design and fabrication for strain rosette sensor array in strain monitoring especially for small-batch equipment.

Acknowledgements
The authors sincerely thank to professor Guoyan Zhou of *East China University of Science and Technology* for her critical discussion during the manuscript preparation.

Authors' Contributions
PY wrote the manuscript; PY and LQ proposed the design conception; LQ and ZG performed the material preparation, array printing and data analyses; YL helped to build the printing equipment; JZ supervised this research. All authors read and approved the final manuscript.

Authors' Information
Peishi Yu is currently an associate professor in mechanical engineering at *Jiangnan University, China*. His research interests include fatigue-fracture mechanics and 3D printed sensors.
Lixin Qi is currently a master candidate in mechanical engineering at *Jiangnan University, China*. His research interests mainly focus on 3D printing sensors.
Zhiyang Guo is currently a PhD candidate in mechanical engineering at *Jiangnan University, China*. His research field is 3D printing in optimizing design and manufacturing.

Yu Liu is currently a professor in mechanical engineering at *Jiangnan University, China*. His research mainly focus on microdevice additive manufacturing.
Junhua Zhao is currently a professor in mechanical engineering at *Jiangnan University, China*. His research interests focus on multi-scale mechanics guided intelligent manufacturing.

Funding
Supported by National Natural Science Foundation of China (Grant No. 11972171), the Sixth Phase of Jiangsu Province "333 High Level Talent Training Project" Second Level Talents, Jiangsu Provincial Natural Science Foundation of China (Grant No. BK20180031), State Key Laboratory of Mechanics and Control of Mechanical Structures, Nanjing University of Aeronautics and Astronautics of China (Grant No. MCMS-E-0422G04), Open Fund of Key Laboratory for Intelligent Nano Materials and Devices of the Ministry of Education NJ2020003 (Grant No. INMD-2021M05), and 111 Project (Grant No. B18027).

Data availability
Data available on request from the authors.

Competing Interests
The authors declare no competing financial interests.

Received: 24 March 2022 Revised: 7 July 2023 Accepted: 10 July 2023
Published online: 15 August 2023

References
[1] T B Sheridan. *Automation, and human supervisory control- telerobotics*. Cambridge MA: The MIT Press, 1992.
[2] C Xu, S Yu, W Wu, et al. Direct ink writing of Fe bone implants with independently adjustable structural porosity and mechanical properties. *Additive Manufacturing,* 2022, 51: 102589.
[3] H Chi, Z Lin, Y Chen, et al. Three-dimensional printing and recycling of multifunctional composite material based on commercial epoxy resin and graphene nanoplatelet. *ACS Appl Mater Interfaces,* 2022, 14(11): 13758–13767.
[4] A Haake, R Tutika, G M Schloer, et al. On-demand programming of liquid metal-composite microstructures through direct ink write 3D printing. *Advanced Materials,* 2022, 34(20): 2200182.
[5] M Saadi, A Maguire, N Pottackal, et al. Direct ink writing: A 3D printing technology for diverse materials. *Advanced Materials,* 2022, 34(28): 2108855.
[6] X Tian. Direct ink writing of 2D material-based supercapacitors. *2D Materials,* 2021, 9(1): 012001.
[7] ACH Tsang, J Zhang, KN Hui, et al. Recent development and applications of advanced materials via direct ink writing. *Advanced Materials Technologies,* 2022, 7(7): 2101358.
[8] L Zhang, W Lee, X Li, et al. 3D direct printing of mechanical and biocompatible hydrogel meta-structures. *Bioactive Materials,* 2022, 10: 48–55.
[9] M Cheng, A Ramasubramanian, MG Rasul, et al. Direct ink writing of polymer composite electrolytes with enhanced thermal conductivities. *Advanced Functional Materials,* 2021, 31(4): 2006683.
[10] N Chaiya, D Daranarong, P Worajittiphon, et al. 3D-printed PLA/PEO blend as biodegradable substrate coating with CoCl2 for colorimetric humidity detection. *Food Packaging and Shelf Life,* 2022, 32: 100829.
[11] K Cao, M Wu, J Bai, et al. Beyond skin pressure sensing: 3D printed laminated graphene pressure sensing material combines extremely low detection limits with wide detection range. *Advanced Functional Materials,* 2022, 32(28): 2202360.
[12] M Di-Oliveira, RG Rocha, LV de Faria, et al. Carbon-black integrated polylactic acid electrochemical sensor for chloramphenicol determination in milk and water samples. *Journal of the Electrochemical Society,* 2022, 169(4): 047517.
[13] K Tyszczuk-Rotko, J Kozak, B Czech. Screen-printed voltammetric sensors-tools for environmental water monitoring of painkillers. *Sensors,* 2022, 22(7): 2437.
[14] R Histed, J Ngo, OA Hussain, et al. Ionic polymer metal composite compression sensors with 3D-structured interfaces. *Smart Materials and Structures,* 2021, 30(12): 125027.
[15] A Kota, A Gogia, AT Neidhard-Doll, et al. Printed textile-based Ag2O-Zn battery for body conformal wearable sensors. *Sensors,* 2021, 21(6): 2178.
[16] X P Hao, C Y Li, C W Zhang, et al. Self-shaping soft electronics based on patterned hydrogel with stencil-printed liquid metal. *Advanced Functional Materials,* 2021, 31(47): 2105481.
[17] J Stulik, J Slauf, R Polansky, et al. Highly sensitive room-temperature ammonia sensors based on single-wall carbon nanotubes modified by PEDOT. *IEEE Sensors Journal,* 2022, 22(4): 3024–3032.
[18] I Mondal, M K Ganesha, A K Singh, et al. Inkjet printing aided patterning of transparent metal mesh for wearable tactile and proximity sensors. *Materials Letters,* 2022, 312: 131724.
[19] T Kant, K Shrivas, K Dewangan, et al. Design and development of conductive nanomaterials for electrochemical sensors: A modern approach. *Materials Today Chemistry,* 2022, 24: 100769.
[20] R Madhavan. Epidermis-like high performance wearable strain sensor for full-range monitoring of the human activities. *Macromolecular Materials and Engineering,* 2022, 307(8): 2200034.
[21] Y Ma, K Liu, L Lao, et al. A stretchable, self-healing, okra polysaccharide-based hydrogel for fast-response and ultra-sensitive strain sensors. *International Journal of Biological Macromolecules,* 2022, 205: 491–419.
[22] X Liu, Z Huang, C Ye, et al. Graphene-based hydrogel strain sensors with excellent breathability for motion detection and communication. *Macromolecular Materials and Engineering*, 2022, 307(8): 2200001.
[23] X He, J Zhou, L Meng, et al. High sensitivity strain sensor based on micro-helix micro taper long period fiber grating. *IEEE Photonics Technology Letters,* 2022, 34(8): 432–435.
[24] Y Wang, Q Wang, S Liu, et al. Lipase induced highly hydrophobic nanofibrillated cellulose film for strain sensor application. *Carbohydrate Polymers,* 2022, 284: 119193.
[25] X Dong, T Song, D Ren, et al. Preparation of wearable strain sensor based on PVA/MWCNTs hydrogel composite. *Materials Today Communications,* 2022, 31: 103278.
[26] W Zhang, S Piao, L Lin, et al. Wearable and antibacterial HPMC-anchored conductive polymer composite strain sensor with high gauge factors under small strains. *Chemical Engineering Journal,* 2022, 435: 135068.
[27] S Li, R Xu, J Wang, et al. Ultra-stretchable, super-hydrophobic and high-conductive composite for wearable strain sensors with high sensitivity. *Journal of Colloid and Interface Science,* 2022, 617: 372–382.
[28] Z Guo, J Xu, Y Chen, et al. High-sensitive and stretchable resistive strain gauges: Parametric design and DIW fabrication. *Composite Structures,* 2019, 223: 110955.
[29] Z Guo, P Yu, Y Liu, et al. High-precision resistance strain sensors of multilayer composite structure via direct ink writing: Optimized layer flatness and interfacial strength. *Composites Science and Technology,* 2021, 201: 108530.
[30] P Yu, L Qi, Z Guo, et al. Arbitrary-shape-adaptable strain sensor array with optimized circuit layout via direct-ink-writing: Scalable design and hierarchical printing. *Materials & Design,* 2022, 214: 110388.
[31] J Muth, D Vogt, R Truby, et al. Embedded 3D printing of strain sensors within highly stretchable elastomers. *Advanced Materials,* 2014, 26(36): 6307-6312.
[32] X Li, Y Yang, B Xie, et al. 3D printing of flexible liquid sensor based on swelling behavior of hydrogel with carbon nanotubes. *Advanced Materials Technologies,* 2019, 4(2): 1800476.
[33] Y Gao, G Yu, T Shu, et al. 3D-printed coaxial fibers for integrated wearable sensor skin. *Advanced Materials Technologies,* 2019, 4(10): 1900504.
[34] Z Guo, P Yu, Y Liu, et al. Pre-fatigue enhancing both long-term stability and sensitivity of direct-ink-writing printed sensors. *International Journal of Fatigue,* 2023, 166: 107237.

Publisher's Note